

# Solvent Effects on Free-Radical Copolymerization Propagation Kinetics of Styrene and Methacrylates

Kun Liang and Robin A. Hutchinson\*

Department of Chemical Engineering, Dupuis Hall, Queen's University, Kingston, Ontario K7L 3N6, Canada

Received May 4, 2010; Revised Manuscript Received June 24, 2010

**ABSTRACT:** Solvent effects on free-radical copolymer composition and propagation kinetics of styrene (ST) with three methacrylates, 2-hydroxyethyl methacrylate (HEMA), glycidyl methacrylate (GMA), and *n*-butyl methacrylate (BMA), are investigated using pulsed-laser polymerization combined with size exclusion chromatography and proton NMR. Three representative solvents, *n*-butanol, toluene, and DMF (*N,N*-dimethylformamide), are selected based on their polarity and structure. It was found that all three solvents have an effect on ST/HEMA copolymer composition compared to bulk copolymerization, with a systematic variation in monomer reactivity ratios observed with solvent polarity. Only butanol affects ST/BMA copolymer composition, and solvent choice has no effect on composition for the ST/GMA system. Butanol increases the composition-averaged copolymerization propagation rate coefficient,  $k_{p, \text{cop}}$ , only for the ST/BMA system, while DMF causes a uniform decrease of  $k_{p, \text{cop}}$  for all three systems and toluene has no observable effect on  $k_{p, \text{cop}}$ . These rate effects are linked to corresponding solvent effects on homopropagation kinetics. It is difficult to reconcile the combined copolymer composition and  $k_{p, \text{cop}}$  data for ST/HEMA systems and for ST/BMA in butanol using the implicit penultimate model of chain-growth, suggesting that H-bonding interactions need to be explicitly considered.

## Introduction

Free radical copolymerization is a useful and mature synthesis methodology to produce materials with diverse functionality in a wide range of media. In order to achieve the desired end-use properties, good control of copolymer composition and, in many cases, copolymerization rate, is required. It is often found that solvent does not affect the relative consumption of the two monomers in homogeneous solution, and thus does not influence copolymer composition. However, this generality starts to break down as the polarity of the monomer and/or solvent increases. For example, Barb<sup>1,2</sup> concluded that the propagation mechanism, and thus copolymer composition, of styrene (ST) and maleic anhydride is affected by solvent choice. Klumperman and co-workers<sup>3,4</sup> also observed the variation in copolymer composition with solvent polarity for copolymerization of ST with both maleic anhydride and with acrylonitrile. As reviewed by Coote et al.,<sup>5</sup> a number of complexation models have been put forth to describe these systems and their deviation from the terminal model, which assumes that radical reactivity only depends on the terminal unit of the growing chain such that the mole fraction of monomer-1 in the copolymer ( $F_1^{\text{inst}}$ ) depends only on monomer mole fractions ( $f_1$  and  $f_2$ , with  $f_1 + f_2 = 1$ ) and the monomer reactivity ratios:<sup>6</sup>

$$F_1^{\text{inst}} = \frac{r_1 f_1^2 + f_1 f_2}{r_1 f_1^2 + 2f_1 f_2 + r_2 f_2^2} \quad (1)$$

where  $r_1 = k_{p11}/k_{p12}$ ,  $r_2 = k_{p22}/k_{p21}$ , and  $k_{pij}$  is the propagation rate coefficient for addition of monomer-*j* to radical-*i*. In contrast to complexation arguments, Harwood<sup>7</sup> proposed the “bootstrap model” based upon the study of ST copolymerized with methacrylic acid, acrylic acid, and acrylamide. It was hypothesized that

solvent does not modify the inherent reactivity of the growing radical, but affects the monomer partitioning such that the concentrations of the two monomers at the reactive site (and thus their ratio) differ from that in bulk.

The most dramatic effects of solvent on copolymer composition involve systems with highly polar monomers such as maleic anhydride, acrylonitrile, and acrylamide. For more “common” systems, such as copolymerization of styrene with acrylates or methacrylates, solvent effects are not observed, or are very subtle. Ito and Otsu<sup>8</sup> studied ST copolymerized with methyl methacrylate (MMA) in various monosubstituted benzene solvents. Fitting their composition data to the terminal model, they reported a small decrease in the values of the ST reactivity ratio ( $r_{\text{ST}}$ ) with increasing solvent polarity, a trend correlated to a small shift of the MMA carbonyl stretching frequency to lower wavenumbers. It was proposed that a more polarized structure of the ester becomes important in the transition state when the solvents become more protic, resulting in increased reactivity. Fujihara et al.<sup>9</sup> extended the study of ST/MMA to a larger range of solvents, including DMF and ethanol (EtOH). They found a small decrease in  $r_{\text{ST}}$  values for copolymerization in DMF compared with benzene, with no change in  $r_{\text{MMA}}$ , a result also reported by Bontà et al.<sup>10</sup> However, the variation results in only very small shifts in composition when examined on a Mayo–Lewis plot of copolymer vs comonomer composition. The decrease observed in EtOH, however, was more significant, with  $r_{\text{ST}}$  decreasing from 0.5 to 0.6 in bulk and other solvents to 0.4 in EtOH.<sup>9</sup> O’Driscoll et al.<sup>11</sup> questioned the statistical significance of these small shifts, while also reporting new results for ST/MMA copolymerization in benzyl alcohol (BzOH) at 30 °C.

In an earlier paper examining the copolymerization of various acrylates and methacrylates with ST, Otsu et al.<sup>12</sup> concluded that the  $r_{\text{ST}}$  value depends on the polar character of the ester substituent on the (meth)acrylate, but not the steric character. Our recent study<sup>13</sup> comparing the bulk copolymerization of ST

\*Corresponding author. E-mail: robin.hutchinson@chee.queensu.ca.

**Table 1. Values of Copolymerization Reactivity Ratios and Homopropagation Rate Coefficients ( $k_p$ , in  $\text{L} \cdot \text{mol}^{-1} \cdot \text{s}^{-1}$ , at 90 °C) for Bulk Copolymerization of Styrene (ST) with 2-Hydroxyethyl Methacrylate (HEMA), Glycidyl Methacrylate (GMA), and *n*-Butyl Methacrylate (BMA)**

	ST/HEMA <sup>13</sup>	ST/GMA <sup>14</sup>	ST/BMA <sup>15</sup>
$r_{\text{ST}}$	$0.27 \pm 0.01$	$0.31 \pm 0.01$	$0.61 \pm 0.03$
$r_{\text{xMA}}$	$0.49 \pm 0.03$	$0.51 \pm 0.02$	$0.42 \pm 0.03$
$s_{\text{ST}}$	$0.38 \pm 0.01$	$0.28 \pm 0.01$	$0.44 \pm 0.05$
$s_{\text{xMA}}$	$1.34 \pm 0.71$	$1.05 \pm 0.23$	$0.62 \pm 0.2$
$k_{p,\text{ST}}$	895	895	895
$k_{p,\text{xMA}}$	6272	2550	1926

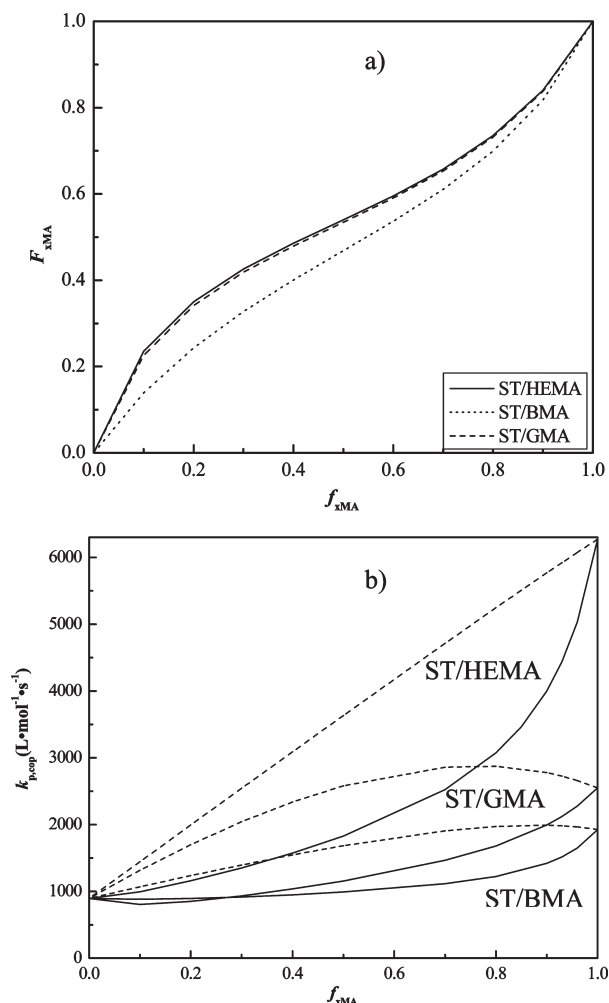


**Figure 1.** (a) Mole fraction methacrylate in copolymer ( $F_{\text{xMA}}$ ) and (b) copolymer propagation rate coefficients ( $k_{p,\text{cop}}$ ) at 90 °C vs mole fraction in monomer mixture ( $f_{\text{xMA}}$ ) for bulk free-radical copolymerization of ST/HEMA, ST/GMA, and ST/BMA, calculated using the coefficients and reactivity ratios in Table 1. Terminal model predictions for  $k_{p,\text{cop}}$  are indicated by the dashed lines and penultimate model fits to experimental data by the solid lines.

with 2-hydroxyethyl methacrylate (HEMA) and glycidyl methacrylate (GMA) to ST/MMA, ST/BMA (*n*-butyl methacrylate) and ST/DMA (*n*-dodecyl methacrylate) systems supports this conclusion: the more polar GMA and HEMA have an increased reactivity toward a styrene radical ( $r_{\text{ST}}$  of 0.27–0.31) compared to the alkyl methacrylates ( $r_{\text{ST}}$  of 0.5–0.6), as summarized in Table 1. Thus, GMA and HEMA produce methacrylate-enriched copolymer in styrene-rich bulk monomer mixtures relative to alkyl methacrylates such as BMA (see Figure 1a). The increased reactivity correlates with a shift of the carbonyl peak to lower

wavenumber as the ester substituent becomes more polar, reducing the electron density at the double bond and increasing the addition rate of the GMA (or HEMA) to a styrene radical relative to BMA.<sup>12,13</sup>

While ST/MMA copolymer composition shows negligible or very minor dependence on solvent choice (with the possible exception of polymerization in alcohols), the same is not true for ST/HEMA. Lebduska et al.<sup>16</sup> used dilatometry to investigate ST/HEMA copolymerizations in DMF, toluene, isopropyl alcohol and *n*-butanol (BuOH). The data were fit using the Mayo–Lewis terminal model, with reactivity ratios found to differ in the polar solvents ( $r_{\text{ST}} = 0.53$  and  $r_{\text{HEMA}} = 0.59$  in DMF, isopropyl alcohol, and BuOH) and the nonpolar toluene ( $r_{\text{ST}} = 0.50$  and  $r_{\text{HEMA}} = 1.65$ ), values that are significantly different from the bulk values of  $r_{\text{ST}} = 0.27$  and  $r_{\text{HEMA}} = 0.48$  reported by Schoonbrood et al.<sup>17</sup> (These latter values provide a good fit to ST/HEMA composition data reported in our recent study.<sup>13</sup>) Sánchez-Chaves et al.<sup>18</sup> analyzed HEMA/ST copolymers produced in DMF using <sup>1</sup>H NMR. The reported monomer reactivity ratios were in good agreement with previous results of Lebduska et al.,<sup>16</sup> with deviations from bulk values<sup>17</sup> qualitatively explained by the bootstrap model.

Most studies of solvent effects on copolymerization kinetics focus solely on copolymer composition. However, it is expected that any solvent influence on monomer reactivity ratios should also affect copolymerization rate. These influences may be complex, as there are many systems for which the terminal model provides a good representation of copolymer composition, but not the variation in the copolymer-averaged propagation rate coefficient,  $k_{p,\text{cop}}$ , as a function of monomer composition. On the basis of previous studies,  $k_{p,\text{cop}}$  can be obtained efficiently and accurately using the PLP/SEC technique, which uses pulsed-laser polymerization (PLP) as a method to determine propagation rate coefficients ( $k_p$ ) via analysis of the resulting polymer molecular weight distributions using size exclusion chromatography (SEC). During PLP experiments, free radicals are initiated from a photoinitiator by the instantaneous laser flash and then propagate and/or terminate with other radicals in the dark period between pulses. A fraction of chains survive the entire dark period to be terminated by the free radicals initiated by the next laser pulse. The resulting dead chains have the same chain length  $L_i$ ,

$$L_i = ik_p[M]t_0; \quad i = 1, 2, 3, \dots \quad (2)$$

where  $[M]$  and  $t_0$  are the total monomer concentration and flash interval, respectively. When the above equation is rearranged, the copolymer-averaged propagation rate coefficient  $k_{p,\text{cop}}$  ( $\text{L} \cdot \text{mol}^{-1} \cdot \text{s}^{-1}$ ) can be deduced from

$$k_{p,\text{cop}} = \frac{MW_0}{1000\rho t_0} \quad (3)$$

where  $MW_0$  is the polymer molecular weight at the first inflection point of the MWD and  $\rho$  ( $\text{g} \cdot \text{mL}^{-1}$ ) is the density of monomer mixture calculated assuming volume additivity. Implicit in eq 3 is that the monomer concentration at the active center is equal to the bulk monomer concentration in solution.

In order to describe  $k_{p,\text{cop}}$  more accurately, Merz et al.<sup>19</sup> first developed the penultimate model:

$$k_{p,\text{cop}} = \frac{\overline{r}_1 f_1^2 + 2f_1 f_2 + \overline{r}_2 f_2^2}{\left(\frac{\overline{r}_1 f_1}{k_{11}}\right) + \left(\frac{\overline{r}_2 f_2}{k_{22}}\right)} \quad (4)$$

When  $\overline{r}_1 = r_1$  and  $\overline{r}_2 = r_2$ , the penultimate unit has no effect on monomer selectivity, a case named the implicit penultimate unit

effect (IPUE) model by Fukuda et al.<sup>20</sup> As a result,  $\overline{k_{11}}$  and  $\overline{k_{22}}$  can be expressed as functions of monomer mole fractions:

$$\overline{k_{11}} = \frac{k_{p11}(r_1f_1 + f_2)}{r_1f_1 + (f_2/s_1)} \quad \overline{k_{22}} = \frac{k_{p22}(r_2f_2 + f_1)}{r_2f_2 + (f_1/s_2)} \quad (5)$$

where  $k_{p11}$  and  $k_{p22}$  are homopolymerization propagation rate coefficients, and  $s_1 = k_{p21}/k_{p11}$  and  $s_2 = k_{p12}/k_{p22}$  are defined as radical reactivity ratios. Deviations from the terminal model are significant for bulk ST/methacrylate systems, as illustrated in Figure 1b for ST/HEMA,<sup>13</sup> ST/GMA,<sup>14</sup> and ST/BMA<sup>15</sup> at 90 °C; the IPUE lines plotted using best-fit  $s$  values from Table 1 provide a good fit to the experimental data measured in these studies.  $k_{p,cop}$  for the ST/HEMA system is significantly greater than values for ST/GMA and ST/BMA system, as the homopropagation rate coefficient for HEMA<sup>21</sup> is more than twice the values for GMA and BMA.

According to the IPUE, solvent effects may influence  $k_{p,cop}$  through six parameters, the homopropagation rate coefficients and radical reactivity ratios in addition to the monomer reactivity ratios that control copolymer composition. Solvent is known to affect homopropagation kinetics for some systems, as has been systematically studied using the PLP/SEC technique and recently reviewed by Beuermann.<sup>22</sup> The magnitude of the change in  $k_p$  is relatively small (up to 20%) for polymerization in solvents which do not undergo specific interaction with either monomer or polymer.<sup>22</sup> We have observed solvent effects of this magnitude for MMA and DMA in 2-heptanone and octyl acetate,<sup>23</sup> but none for BMA in the same solvents<sup>23</sup> or for GMA in xylene.<sup>14</sup> A significant solvent effect is observed for ST homopropagation in DMF, with  $k_p$  reduced by 15–25% compared to bulk polymerization.<sup>24</sup>

The effect of solvent on homopropagation kinetics can be more pronounced for systems with H-bonding. For ST,  $k_p$  values were found to increase by 50% in BzOH,<sup>25</sup> although neither EtOH nor methanol (MeOH) had an effect on ST homopropagation.<sup>26</sup> The same two studies found that alcohols have a more uniform and larger effect on  $k_p$  values for alkyl methacrylates, with the  $k_p$  of MMA 70% higher in 70 mol % BzOH compared to bulk values at 25 °C,<sup>25</sup> and the  $k_p$  of MMA increased by up to 40% in MeOH and EtOH.<sup>26</sup> Similarly, Beuermann reported that the  $k_p$  of BMA in *n*-butanol ( $[BMA] = 0.8 \text{ mol} \cdot \text{L}^{-1}$ ) is 45% higher than that in bulk at 80 °C.<sup>27</sup> Raman spectroscopy indicated a corresponding shift in the position of the carbonyl peak, with the bimodal structure (a second peak occurring at lower wavenumber of about  $1700 \text{ cm}^{-1}$ ) that occurs in the presence of butanol attributed to the BMA carbonyl group interacting with the solvent OH group, reducing electron density at the double bond and increasing  $k_p$ .<sup>22,27</sup>

On the basis of these findings, it is not surprising that solvent choice can also influence the homopropagation kinetics of hydroxy-functional methacrylates. Beuermann and Nelke<sup>28</sup> reported that  $k_p$  values for hydroxypropyl methacrylate (HPMA) are 40% lower in THF than the corresponding bulk values. Raman spectroscopy was used to show that the addition of THF reduces the bimodal nature of the carbonyl peak seen for bulk HPMA, disrupting the extent of monomer–monomer H-bonding.<sup>22,28</sup> This effect was not observed in toluene or BzOH, solvents that did not significantly affect HPMA propagation.<sup>28</sup> Buback and Kurz<sup>21</sup> also found only a negligible change for the  $k_p$  of HEMA in 50 vol % *n*-butanol.

There is significantly less work in the literature that extends the study of solvent choice on  $k_p$  to copolymerization systems. Fukuda et al.,<sup>29</sup> using the rotating sector technique, found no observable difference in  $k_{p,cop}$  values for ST/MMA (a system with a significant penultimate effect) measured in bulk and in toluene, a result also found by Olaj and Schnöll-Bitai<sup>30</sup> using the

PLP/SEC technique. This result is not surprising; as discussed above, neither homopropagation rate coefficients nor  $r$  values exhibit a strong solvent effect in toluene. For ST/MMA in BzOH with  $f_{ST} = 0.5$ , however,  $k_{p,cop}$  increases by 65% as solvent level is increased from 0 to 75%.<sup>11</sup> This increase is comparable to what is found for MMA  $k_p$  (70%), but larger than that observed for ST  $k_p$  (40–50%).<sup>25</sup> The findings were interpreted assuming that the solvent complexes with MMA radicals more strongly than with ST radicals; as mentioned previously, the  $r$  values for the system are almost unchanged.<sup>11</sup> No other studies could be found that simultaneously consider the effect of solvent on both copolymer composition and  $k_{p,cop}$ .

As summarized in Figure 1, we have systematically studied copolymer chain-growth kinetics for styrene–(ST) methacrylate (xMA) systems in bulk, examining the effect of methacrylate ester group (denoted by x) and temperature on polymer composition and propagation kinetics for copolymers of *n*-butyl methacrylate (BMA) and ST,<sup>15</sup> 2-hydroxyethyl methacrylate (HEMA) and ST,<sup>13</sup> and glycidyl methacrylate (GMA) and ST<sup>14</sup> via PLP/SEC, with copolymer composition determined via proton NMR. These kinetic studies were part of a larger effort to understand and model the complexities of the high temperature free-radical solution process used to make acrylic resins for solvent-borne automotive coatings.<sup>31,32</sup> As many reactions in industry are carried out in solvents rather than in bulk, it is useful to extend this investigation to solution copolymerization using a nonpolar (toluene), a polar (DMF), and an H-bonding (*n*-butanol) solvent. The determination of both copolymer composition and  $k_{p,cop}$  provides new insight into the ability of the IPUE model to describe copolymerization chain growth in solution for systems with significant H-bonding effects.

## Experimental Section

BMA (99% purity containing 10 ppm monomethyl ether hydroquinone (MEHQ)), GMA (97% purity containing 100 ppm MEHQ), HEMA (97% purity containing 200–220 ppm MEHQ), styrene (99% purity, containing 10–15 ppm of 4-*tert*-butylcatechol), *n*-butanol (99% purity), toluene (99.8% purity), DMF (99.8% purity), photoinitiator DMPA (2,2-dimethoxy-2-phenylacetophenone, 99% purity), chloroform-*d* (containing 99.9 atom % D) and anhydrous DMSO-*d*<sub>6</sub> (dimethyl-*d*<sub>6</sub> sulfide, containing 99.9 atom % D) were all obtained from Sigma-Aldrich and used as received.

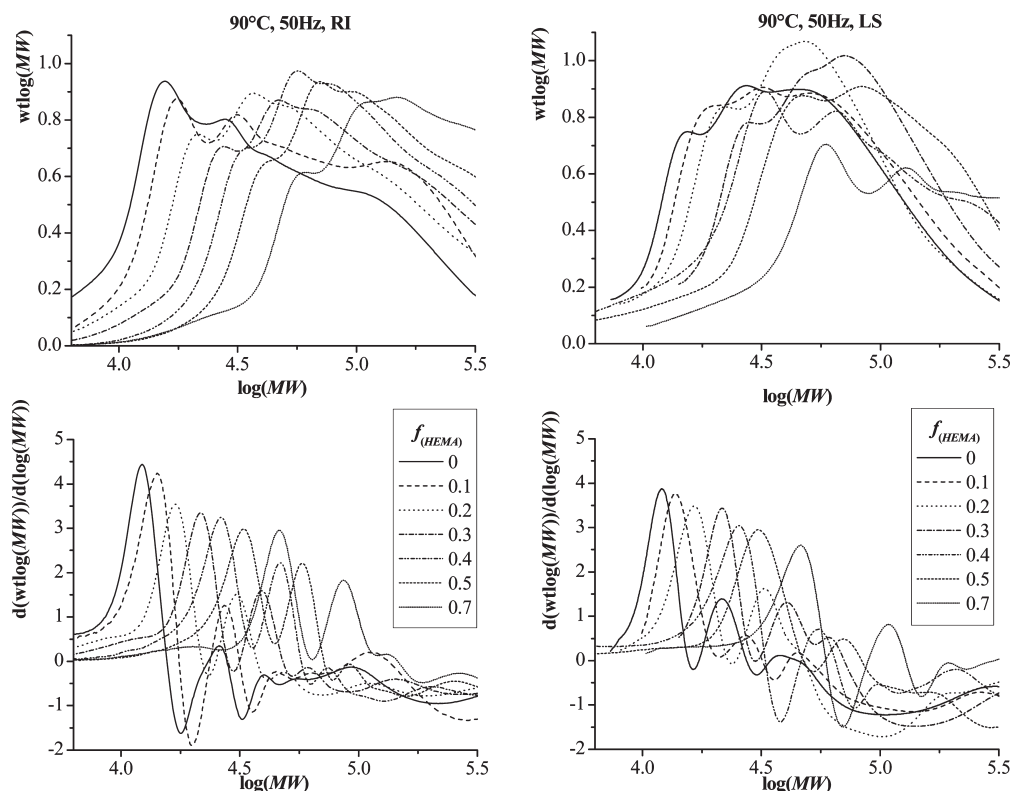
Low conversion polymerizations were conducted in a pulsed laser setup consisting of a Spectra-Physics Quanta-Ray 100 Hz Nd:YAG laser that is capable of producing a 355 nm laser pulse of duration 7–10 ns and energy of 1–50 mJ per pulse. The laser beam is reflected twice (180°) to shine into a Hellma QS165 0.8 mL jacketed optical sample cell used as the PLP reactor. A digital delay generator (DDG, Stanford Instruments) is attached to the laser in order to regulate the pulse output repetition rate at a value between 10 and 100 Hz. Monomer mixtures in solvents with  $5 \text{ mmol} \cdot \text{L}^{-1}$  DMPA photoinitiator were added to the cylindrical quartz cell and exposed to laser energy, with temperature controlled by a circulating oil bath. Experiments were run at 90 °C, with styrene fraction in the monomer mixture varied between 0 and 100%. Monomer conversions, measured by gravimetry, were kept below 5% to avoid significant composition drift. The polymers produced by PLP were also used for composition analysis by proton NMR, using procedures described previously.<sup>13–15</sup>

Polymers produced by PLP were used to determine  $k_{p,cop}$  from analysis of polymer molecular weight distributions (MWD) measured by size exclusion chromatography (SEC). The resulting samples of poly(ST/HEMA) from PLP were precipitated in diethyl ether, while the samples of poly(ST/GMA) and poly(ST/BMA) were precipitated in methanol and dried as described previously.<sup>13–15</sup> Molecular weight distributions were measured with a Waters 2960 separation module connected to a Waters 410



**Table 2.** Parameters for Calculation of  $k_{p, \text{cop}}$  from SEC Analysis of PLP-Generated Copolymer Samples of Styrene with Methacrylates in Solution

species	density $\rho$ ( $\text{g} \cdot \text{mL}^{-1}$ )	$dn/dc$ ( $\text{mL} \cdot \text{g}^{-1}$ )	Mark–Houwink parameters		ref
			$K \times 10^4$ ( $\text{dL} \cdot \text{g}^{-1}$ )	$a$	
styrene	$0.9193 - 0.000665T/^{\circ}\text{C}^{33}$	$0.180^{36}$	1.14	0.716	37
HEMA	$1.0920 - 0.00098T/^{\circ}\text{C}^{21}$	$0.0556^{13}$	2.39	0.537	13
GMA	$1.094728 - 0.001041T/^{\circ}\text{C}^{34}$	$0.093^{14}$	2.78	0.537	34
BMA	$0.91454 - 0.000964T/^{\circ}\text{C}^{35}$	$0.080^{36}$	1.48	0.664	37
toluene	$0.88575 - 0.000941T/^{\circ}\text{C}^{38}$				
<i>n</i> -butanol	$0.8398 - 0.00119T/^{\circ}\text{C}^{27}$				
DMF	$1.235026 - 0.000972T/^{\circ}\text{C}^{39}$				

**Figure 2.** MWDs (top) and corresponding first derivative (bottom) plots obtained for styrene/2-hydroxyethyl methacrylate (HEMA) copolymer produced by PLP in 50 vol % DMF at 90 °C and 50 Hz, as measured by RI (left) and LS (right) detectors. Monomer compositions are given as mole fraction HEMA ( $f_{\text{HEMA}}$ ).

differential refractometer (DRI) and a Wyatt Instruments Dawn EOS 690 nm laser photometer multiangle light scattering (LS) detector. Tetrahydrofuran (THF) was used as eluent at a flow rate of  $1 \text{ mL} \cdot \text{min}^{-1}$  through the four Styragel columns (HR 0.5, 1, 3, 4) maintained at 35 °C. The DRI detector was calibrated by 10 narrow polydispersity polystyrene standards in a broad MW range (870–355000 Da), and the LS detector was calibrated by toluene as recommended by the manufacturer.

The parameters necessary to estimate  $k_{p, \text{cop}}$  from SEC data are summarized in Table 2, with monomer densities calculated as a function of temperature, the refractive index ( $dn/dc$ ) values required for interpretation of LS results, and Mark–Houwink parameters required in order to analyze the output from the RI detector. The polymer MWD is calculated using a copolymer composition-weighted average of the homopolymer values from the RI detector, and a composition-weighted  $dn/dc$  value for analysis of the LS results, as done previously.<sup>13–15</sup> Agreement between the two detectors was good (within 10%) over a wide range of  $MW_0$  values, between  $5 \times 10^3$  and  $1 \times 10^5$  Da. Reported  $k_{p, \text{cop}}$  values are calculated using the LS results, as previous studies suggest these results are more accurate for the ST/GMA<sup>14</sup> and ST/HEMA<sup>13</sup> systems.

Monomer mixtures in bulk and solution were examined using a Nicolet FT-IR spectrometer at room temperature to examine for

the effect of H-bonding on the methacrylate carbonyl peak in the range of  $1700$  to  $1720 \text{ cm}^{-1}$ , with spectra normalized according to peak height.

## Results and Discussion

A series of PLP/SEC experiments were performed at 90 °C for the ST/HEMA, ST/GMA, and ST/BMA systems in *n*-butanol (BuOH), DMF and toluene solvents, with solvent levels at 25 and 50 vol %. Most experiments were conducted at a laser repetition rate of 50 Hz, with a few at 25 and 33 Hz; as found previously,<sup>13–15</sup>  $k_{p, \text{cop}}$  estimates show no systematic variation with pulse repetition rate. Except for the solvent presence, the experimental conditions are identical to those used in the recent PLP/SEC studies of bulk copolymerization.<sup>13–15</sup> Proton NMR was used to determine composition of the low conversion samples. The complete set of experimental results, both copolymer composition and  $k_{p, \text{cop}}$  data, is available as Supplemental Data (Tables S1–S3). Figure 2 shows a typical set of MWDs and corresponding first-derivative plots. The  $k_{p, \text{cop}}$  values were determined using the primary inflection points from the first-derivative curves calculated from the MWD, with the data considered to be valid only if a secondary inflection point was observed at a MW

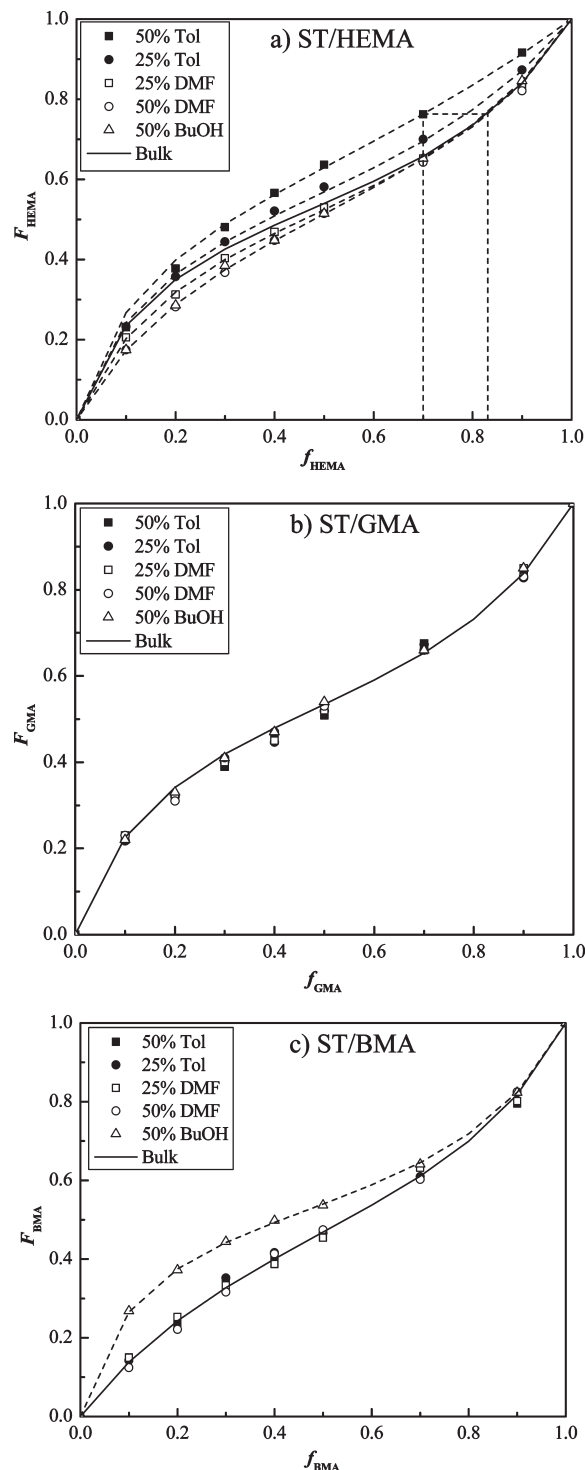
value twice that of the primary point. The data shown are as determined from analysis of the output of the LS detector, which was in good agreement (within 10%) of the estimates from the RI detector (see Tables S1–S3). Note that it was only possible to measure  $k_{p,\text{cop}}$  of ST/HEMA for systems with  $f_{\text{HEMA}}$  of 0.7 or lower, as copolymers produced at higher HEMA fraction were not THF-soluble.

The analysis of the data is performed assuming that monomer concentrations in the domain of the active radical are the same as in bulk solution; i.e., that no monomer partitioning occurs. Monomer reactivity ratios are estimated based upon the terminal model of polymerization chain-growth kinetics,<sup>6</sup> while  $k_{p,\text{cop}}$  data are analyzed according to the IPUE representation.<sup>20</sup> When solvent effects are important, as found for some of the experimental systems examined in this work, these assumptions have been questioned. As discussed in the introduction, a variety of partitioning and complexation models have been proposed,<sup>5,7</sup> and it has been argued that solvent effects indicate an explicit penultimate unit effect on propagation.<sup>5,7,40</sup> However, as shown below, we find that the widely accepted models of copolymerization provide a good representation of the data for most cases. The solution polymerization results presented here build on the bulk studies of ST/BMA, ST/GMA and ST/HEMA propagation kinetics summarized in Figure 1, with corresponding IPUE coefficients at 90 °C summarized in Table 1. For reasons that will become apparent, the effect of solvent on copolymer composition and on  $k_{p,\text{cop}}$  will be discussed separately before considering the implications that the combined set of measurements have on our understanding of copolymerization propagation kinetics.

**Copolymer Composition.** Figure 3 plots copolymer composition as a function of monomer composition, as determined in low conversion ST/xMA experiments at 90 °C conducted with 25 or 50 vol % solvent present. The solid line in each plot is calculated assuming terminal kinetics and using the reactivity ratios determined from analysis of the corresponding bulk systems summarized in Table 1.

For ST/HEMA (Figure 3a), the presence of BuOH and DMF leads to the formation of copolymer enriched in ST relative to the bulk case for copolymerizations conducted with low HEMA content ( $f_{\text{HEMA}} < 0.6$ ); the copolymer composition converges to that found for copolymerizations in bulk with higher HEMA content ( $f_{\text{HEMA}} > 0.6$ ). The opposite trend is observed for copolymerizations performed in toluene: HEMA-rich copolymer is formed (relative to the bulk system) for mixtures with medium and high HEMA content ( $f_{\text{HEMA}} > 0.2$ ), with the copolymer composition the same as found for bulk mixtures with low HEMA content. The data set at each solvent level has been fit to the Mayo–Lewis equation via nonlinear parameter estimation, with results (including 95% confidence intervals) summarized in Table 3. The observed shifts in copolymer composition for copolymerization in butanol and DMF are best fit by keeping  $r_{\text{HEMA}}$  constant at the bulk value and increasing  $r_{\text{ST}}$ , while the results obtained for polymerization in toluene are best fit with  $r_{\text{ST}}$  relatively constant and increasing  $r_{\text{HEMA}}$ .

In contrast to the ST/HEMA results and despite the polar nature of GMA, the copolymer composition of ST/GMA is not affected by solvent choice to any significant effect (Figure 3b). ST/BMA composition (Figure 3c) is unchanged by DMF or toluene solvent, but is significantly affected by the addition of BuOH, a result captured by a large decrease in  $r_{\text{ST}}$  ( $r_{\text{ST}} = 0.21 \pm 0.02$ ,  $r_{\text{BMA}} = 0.38 \pm 0.04$  compared to  $r_{\text{ST}} = 0.61 \pm 0.03$  and  $r_{\text{BMA}} = 0.42 \pm 0.03$  in bulk). The results summarized in Figure 3 are in good agreement with the ST/HEMA and ST/MMA literature discussed previously: with the exception of alcohols, solvent has, at most,

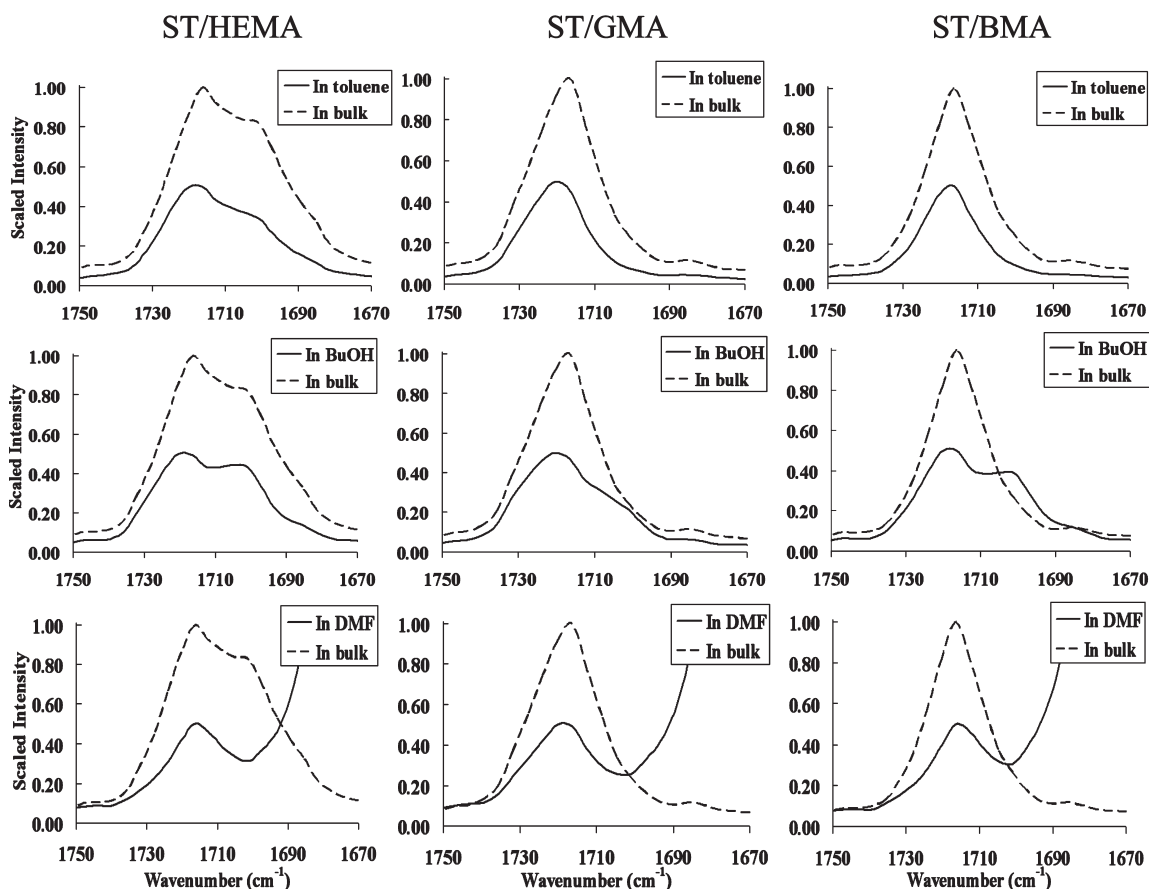


**Figure 3.** Copolymer composition data for low-conversion (a) styrene/HEMA, (b) styrene/GMA, and (c) styrene/BMA solution copolymerizations, plotting mole fraction methacrylate in copolymer ( $F_{\text{xMA}}$ ) as a function of methacrylate mole fraction in the monomer phase ( $f_{\text{xMA}}$ ). The solid curve in each plot is the prediction of the terminal copolymerization model with bulk monomer reactivity ratios from Table 1.

a minor effect on reactivity ratios for copolymerization of ST with alkyl methacrylates (MMA, BMA), but has a startling effect on the copolymerization of ST with HEMA. In addition, we find that ST/GMA copolymer composition (and thus reactivity ratios) is rather insensitive to solvent choice, and that the variation in reactivity ratios for the ST/HEMA

**Table 3. Monomer Reactivity Ratios of ST/HEMA in Solution, Determined by Fit of the Terminal Model to Experimental Data Shown in Figure 3a**

		toluene		DMF		butanol
	bulk <sup>13</sup>	25 vol %	50 vol %	25 vol %	50 vol %	50 vol %
$r_{ST}$	0.27	$0.26 \pm 0.02$	$0.23 \pm 0.02$	$0.35 \pm 0.01$	$0.45 \pm 0.03$	$0.44 \pm 0.03$
$r_{HEMA}$	0.49	$0.66 \pm 0.08$	$1.09 \pm 0.18$	$0.49 \pm 0.04$	$0.53 \pm 0.10$	$0.54 \pm 0.10$

**Figure 4.** FT-IR spectra comparison of comonomer mixtures (1:1 mol ratio) of ST/HEMA (left column), ST/GMA (middle column) and ST/BMA (right column) at room temperature in bulk and in: 50 vol % toluene (top row), butanol (middle row), and DMF (bottom row) solutions.

system changes systematically with solvent level, a result not reported in previous studies.

Previous ST/xMA studies have explained the effect of solvent on copolymer composition using both reactivity (H-bonding affecting the relative reactivity of monomers to radicals) and physical (the ratio of monomer concentrations at the reactive site is different than in the bulk mixture) arguments. Let us first consider the physical bootstrap effect by examining Figure 3a at a specific  $f_{HEMA}$  value of 0.70, as marked on the plot. The corresponding HEMA fraction in the copolymer formed in BuOH and DMF is the same as measured in bulk, with  $F_{HEMA} = 0.62$ . However, the experimentally determined  $F_{HEMA}$  value is 0.75 in 50 vol % toluene solution. Assuming that this difference in composition can be attributed solely to the bootstrap effect (HEMA monomer is preferentially partitioned around the HEMA-rich copolymer chains in the nonpolar toluene solvent) and that the bulk reactivity ratios are true values, the plot indicates that the fraction of HEMA in the monomer mixture found locally around the radicals must be enriched to 0.82. Meanwhile, in the polar solvents BuOH and DMF, ST monomer preferentially partitions to the ST-rich copolymer chains, an effect that diminishes as the HEMA fraction is increased in the monomer mixture (and in the copolymer that is formed).

While often used to explain copolymer composition in polar systems, however, it is difficult to use only the bootstrap effect to explain these ST/HEMA results. One reason is that the explanation is inconsistent with the  $k_{p, cop}$  results (presented later). In addition, no similar influence of solvent on copolymer composition is observed for the relatively polar ST/GMA system, from which it can be concluded that it is an effect specific to H-bonding.

Thus, let us consider solvent effects on the monomer relative reactivity. As discussed by Beuermann<sup>22</sup> and Ito and Otsu,<sup>8,12</sup> IR spectroscopy can be used as a probe to study monomer and solvent interactions. From the FT-IR spectra shown as Figure 4, a shoulder at  $\sim 1700\text{ cm}^{-1}$  for the carbonyl region of xMA is observed in bulk ST/HEMA that is not present for bulk ST/GMA or ST/BMA. The shoulder indicates hydrogen bonding between the monomer OH group and carbonyl O atom that strengthens the positive partial charges at the carbonyl C atom and at the double bond, as shown schematically in Figure 5, leading to a significant charge transfer in the transition state of propagation. When toluene is added to the system, the HEMA H-bonding is still distinct but diluted, such that the monomer reactivity toward a ST radical remains unchanged from bulk (see  $r_{ST}$  values in Table 3). However, the  $r_{HEMA}$  value

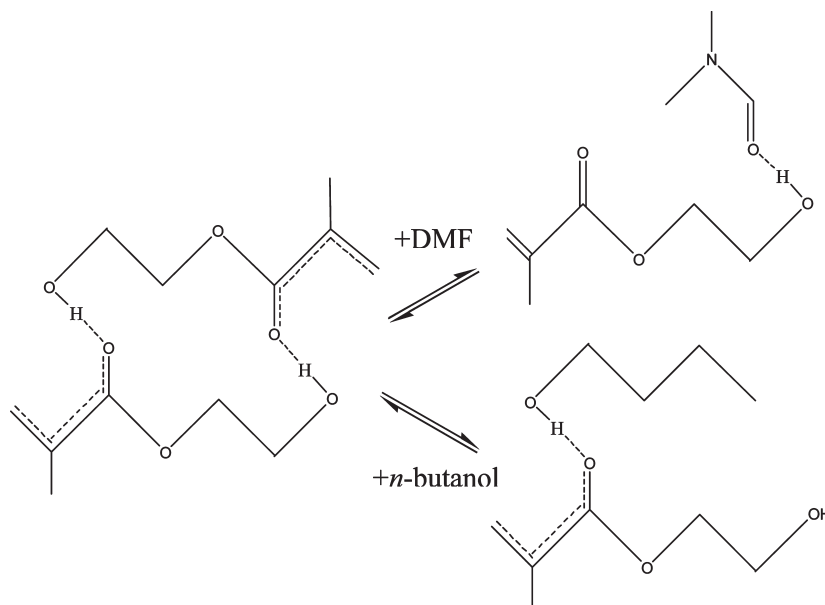


**Figure 5.** Schematic representation of H-bonding between two HEMA monomer molecules in bulk (left), compared to between DMF and HEMA or between *n*-butanol and HEMA in solution.

changes significantly, to the point where HEMA monomer addition to a HEMA radical is favored over ST addition ( $r_{\text{HEMA}} > 1$ ). Generally speaking, when charge transfer in the transition state is significant, the stability of the charge transfer species is affected by the polarity of the solvent,<sup>5</sup> which can explain why toluene has an effect on the ST/HEMA reactivity ratios, but no influence on the ST/GMA system.

The shoulder for HEMA at  $1708\text{ cm}^{-1}$  disappears in the presence of DMF for the ST/HEMA mixture (see Figure 4), although there is interference from the strong DMF peak. This behavior is similar to what was reported for 2-hydroxypropyl methacrylate (HPMA) in THF,<sup>28</sup> and it is an indication that the HEMA–HEMA interactions are disrupted and replaced by hydrogen bonding between the DMF carbonyl oxygen and the HEMA hydroxyl group, as shown schematically in Figure 5. When BuOH is added to the system the  $1708\text{ cm}^{-1}$  peak for HEMA remains unchanged or is slightly enhanced, as observed by Beuermann and Nelke<sup>28</sup> for HPMA in BzOH, suggesting that some of the HEMA–HEMA H-bonding is replaced by HEMA–BuOH H-bonding (see Figure 5). In both cases, the disruption of hydrogen bonding between HEMA molecules is consistent with the decreased rate of monomer addition to ST radicals compared to bulk copolymerization; for example, the value of  $r_{\text{ST}}$  required to fit the copolymer composition in 50 vol % DMF (see Figure 3a and Table 3) increases to 0.45, a value that is more typical for ST with alkyl methacrylates.<sup>15</sup> These spectra suggest that BuOH and DMF affect ST/HEMA copolymer composition through specific interactions with HEMA, while toluene works through a polarity effect.

**Copolymerization Propagation Coefficient ( $k_{\text{p, cop}}$ ).** Figure 6 plots the values of  $k_{\text{p, cop}}$  at  $90^\circ\text{C}$  as a function of monomer composition, determined from low conversion ST/xMA experiments in 25 and 50 vol % toluene, 25 and 50 vol % DMF, and 50 vol % BuOH. The solid lines drawn in Figure 6 are calculated assuming implicit penultimate kinetics and using the monomer and radical reactivity ratios and homopropagation rate coefficients determined from analysis of the corresponding bulk systems summarized in Table 1. What can be immediately observed is that the  $k_{\text{p, cop}}$  values measured in toluene are in very good agreement with those for the bulk ST/xMA systems for all

three methacrylates, in agreement with previous ST/MMA studies.<sup>29,30</sup>

The  $k_{\text{p, cop}}$  values measured in DMF are lower than the bulk values throughout most of the composition range, independent of whether experiments were conducted with 25 or 50 vol % DMF. This difference is clearly observed for ST homopolymerization ( $f_{\text{xMA}} = 0$ ); in agreement with previous literature,<sup>24</sup> our PLP results indicate that  $k_{\text{p}}$  values for ST are reduced by 20% in DMF compared with bulk. This result can be explained by a reversible complexation between DMF and the aromatic group of styrene, similar to the arguments used by Kamachi et al.<sup>41</sup> to explain the aromatic solvent effect on polymerization of vinyl acetate. The decrease in  $k_{\text{p, cop}}$  values in DMF relative to bulk becomes smaller as the methacrylate fraction in the ST/BMA and ST/GMA systems increases, with no solvent effect observed for homopolymerization of BMA or GMA values in DMF. For ST/HEMA, however, the difference between  $k_{\text{p, cop}}$  and the bulk system increases in magnitude with increasing HEMA fraction in the monomer phase. This trend strongly suggests that the HEMA  $k_{\text{p}}$  value is significantly reduced in DMF, as would be expected based upon the 40% decrease of HPMA  $k_{\text{p}}$  in THF reported in the literature.<sup>28</sup>

The immediate question that arises is whether or not the penultimate model will provide a fit to the ST/xMA  $k_{\text{p, cop}}$  data in DMF using the  $r$  and  $s$  values (for bulk polymerization) from Table 1, after adjusting the end point  $k_{\text{p}}$  values to account for solvent effects. The dashed lines in each figure indicate that this is indeed the case; in all cases the IPUE provides a good representation of the data. Thus,  $k_{\text{p, cop}}$  values can be predicted for solution polymerization using bulk  $r$  and  $s$  copolymerization results not only for systems that exhibit no solvent effects (ST/xMA in toluene), but also for solvents that influence homopropagation behavior. The result is surprising since, as shown in Figure 3a, H-bonding has a significant effect on ST/HEMA copolymer composition in both toluene and DMF solution.

BuOH is not only a polar solvent but also carries a hydroxyl group. Thus, it is interesting to look into its effect on ST/xMA copolymerization. For ST/GMA (Figure 6b), the  $k_{\text{p, cop}}$  curve is in good agreement with the bulk and



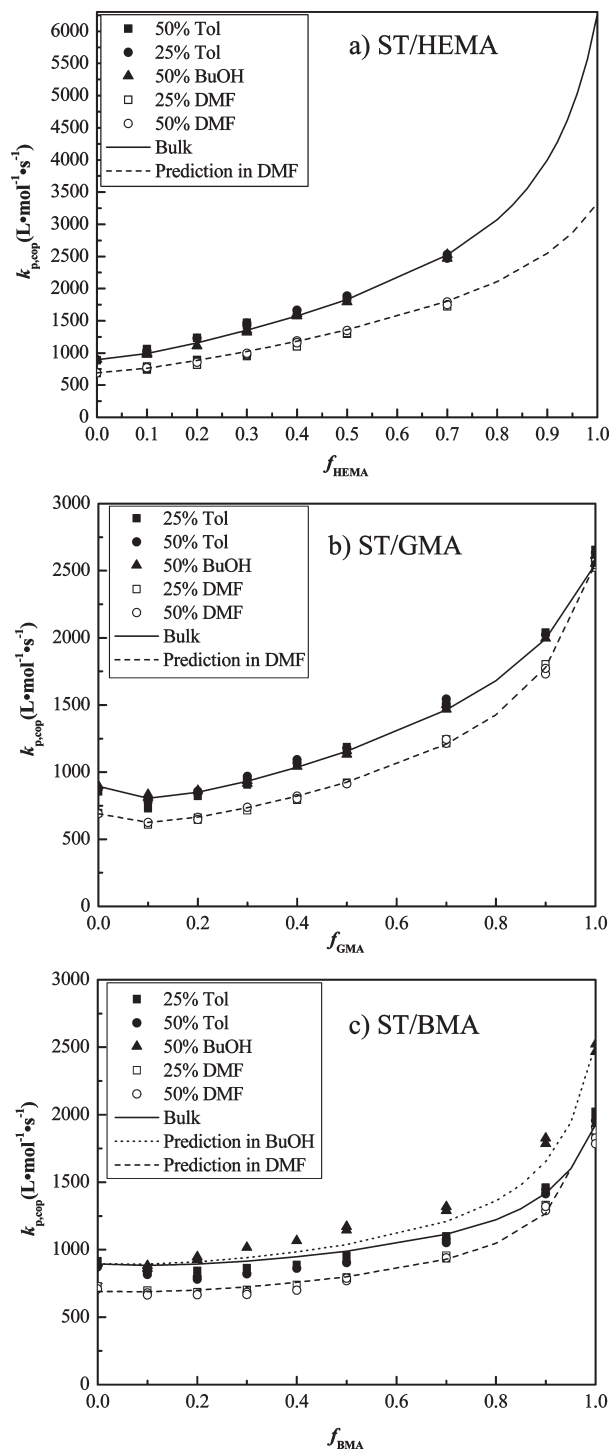


**Figure 6.** Experimental  $k_{p, \text{cop}}$  ( $\text{L} \cdot \text{mol}^{-1} \cdot \text{s}^{-1}$ ) values determined by SEC analysis of (a) styrene/HEMA, (b) styrene/GMA, and (c) styrene/BMA copolymers produced via PLP experiments at 90 °C, plotted as a function of monomer mole fraction. Lines indicate predictions according to the implicit penultimate unit effect model with  $r$  and  $s$  values taken from bulk studies (Table 1). Values for  $k_{p, \text{ST}}$  in DMF,  $k_{p, \text{HEMA}}$  in DMF and  $k_{p, \text{BMA}}$  in BuOH adjusted according to experimental data (see text).

toluene solution systems, and well represented using the bulk values for homopropagation kinetics and IPUE reactivity ratios summarized in Table 1. (In agreement with the study of ST homopolymerization in EtOH and methanol,<sup>29</sup> BuOH has no effect on ST homopolymerization kinetics.) Figure 6a also indicates that ST/HEMA  $k_{p, \text{cop}}$  is the same in BuOH as

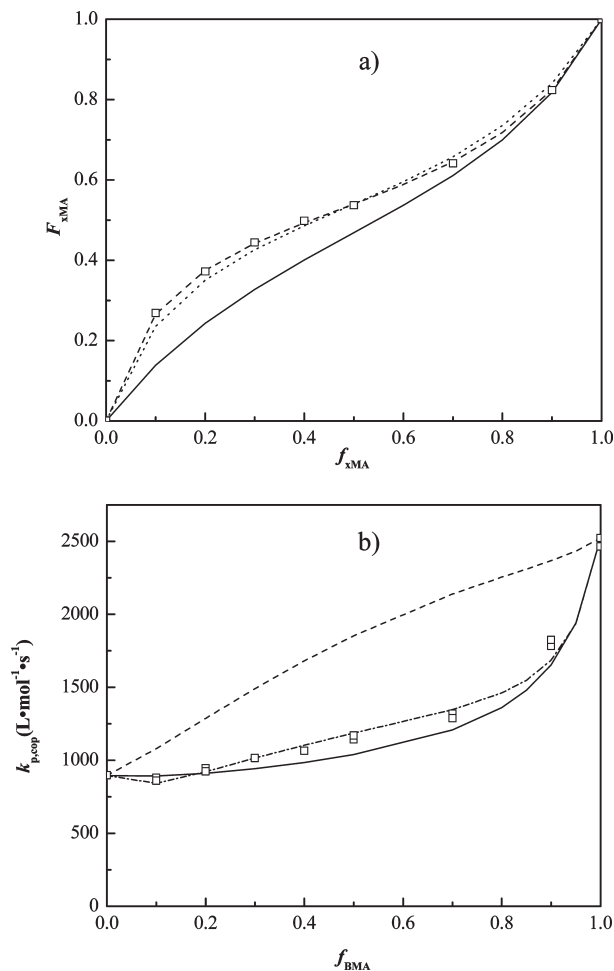


**Figure 7.** (a) Copolymer composition ( $F_{x\text{MA}}$ ) and (b) 90 °C  $k_{p, \text{cop}}$  results for ST/BMA copolymerization in 50 vol % BuOH solution (symbols) compared to predictions calculated using: IPUE reactivity ratios determined in bulk (—);  $s$  values from bulk and  $r$  values fit to copolymer composition data in BuOH (---); and  $s$  values fit to BuOH  $k_{p, \text{cop}}$  data with  $r$  values fit to copolymer composition data in BuOH (· · ·). All lines calculated with  $k_{p, \text{BMA}} = 2523 \text{ L} \cdot \text{mol}^{-1} \cdot \text{s}^{-1}$ , as measured in BuOH solution. The dotted line in a) represents copolymer composition obtained in the bulk ST/HEMA system.

in bulk and toluene for monomer mixtures containing up to 70 mol % HEMA; this result suggests that HEMA homopolymerization  $k_p$  values are the same in BuOH as in bulk, in agreement with previous results for HPMa in BzOH<sup>28</sup> and for HEMA in EtOH.<sup>21</sup>

For ST/BMA (Figure 6c), BuOH enhances the homopropagation of BMA by 30% at 90 °C, in agreement with the results presented by Beuermann.<sup>27</sup> As shown in the spectrum in Figure 4, the addition of BuOH to the system leads to H-bonding between the BuOH and BMA, making the monomer act in a fashion similar to HEMA. The line plotted in Figure 6c makes this adjustment to  $k_{p, \text{BMA}}$ , but keeps the  $r$  and  $s$  values set to bulk values. The experimental data are close to the IPUE predictions using the  $r$  and  $s$  values determined in bulk. A small adjustment (setting  $s_{\text{ST}} = 0.49$  and  $s_{\text{BMA}} = 0.80$ ) within the uncertainty range reported in Table 1, provides an excellent fit to the data (curve not shown). As for the ST/HEMA data, this good representation is surprising, as BuOH significantly affects copolymer composition and corresponding  $r$  estimates (Figure 3c).

**Combined Data Sets.** We now turn to the full set of composition and  $k_{p, \text{cop}}$  results summarized in Figures 3 and 6. For ST/BMA and ST/GMA, the curves calculated



using the Table 1 IPUE parameter values from bulk copolymerization provide a good representation of the  $k_{p, \text{cop}}$  values measured in toluene as well as copolymer composition data. The same can be said for the ST/GMA results measured in BuOH. Bulk  $r$  and  $s$  values also provide a good fit to the copolymer composition and  $k_{p, \text{cop}}$  values measured in DMF for ST/BMA and ST/GMA, after decreasing the  $k_{p, \text{ST}}$  value at 90 °C by 20% (to  $691 \text{ L} \cdot \text{mol}^{-1} \cdot \text{s}^{-1}$ ) to match the homopolymerization PLP/SEC results. Thus, 5 out of the 9 systems are easily understood and represented by the IPUE model of copolymerization kinetics. The same, however,

cannot be said for ST/BMA polymerized in BuOH and for the complete set of ST/HEMA solution results.

Figure 7 plots both the copolymer composition and  $k_{p, \text{cop}}$  results for ST/BMA in BuOH. The composition data (Figure 7a) can be fit by the terminal model, but using a different set of monomer reactivity ratios ( $r_{\text{ST}} = 0.21$ ,  $r_{\text{BMA}} = 0.38$ ) compared to the values for the bulk system ( $r_{\text{ST}} = 0.61$ ,  $r_{\text{BMA}} = 0.42$ ). As discussed by Fujihara et al.<sup>9</sup> for ST/MMA in EtOH, H-bonding of the ester with the alcohol reduces the electron density of the alkyl methacrylate double bond compared to in bulk or other solvents, making it more reactive toward ST radicals. Also shown is the copolymer composition curve plotted using  $r$  values estimated for ST/HEMA bulk ( $r_{\text{ST}} = 0.27$ ,  $r_{\text{HEMA}} = 0.48$ ). The copolymer composition curves (and reactivity ratio estimates) for ST/BMA in BuOH and ST/HEMA in bulk are quite similar, suggesting that the influence of H-bonding on relative reactivity is also similar.

The ST/BMA  $k_{p, \text{cop}}$  experimental data measured in BuOH are reasonably well represented by the IPUE model using the  $r$  and  $s$  values determined in bulk. Of course, one would consider that the  $r$  values fit to the ST/BMA composition data in BuOH should be used in eqs 4 and 5 to calculate  $k_{p, \text{cop}}$  for this system. As shown in Figure 7b, however, this adjustment causes some significant deviation between the experimental data and the IPUE predictions. It is possible to refit the IPUE model to the data using the new  $r$  values and with  $s_{\text{ST}} = 0.32 \pm 0.02$  and  $s_{\text{BMA}} = 0.27 \pm 0.03$  (compared to the Table 1 values of  $0.44 \pm 0.05$  and  $0.62 \pm 0.2$ ). However, the shape of the best-fit IPUE line does not match the data particularly well, suggesting that an explicit consideration of H-bonding effects is needed.

It is also difficult to come up with a cohesive description of the ST/HEMA copolymerization propagation kinetics. As found for ST/BMA in BuOH, the ST/HEMA  $r$  and  $s$  values measured in bulk provide a good match to  $k_{p, \text{cop}}$  data according to the IPUE model (Figure 6a) but the bulk  $r$  values do not describe copolymer composition data (Figure 3a). To examine this result further, we calculate  $k_{p, \text{cop}}$  curves using the  $r$  values from Table 3 (estimated from the terminal model fit to copolymer composition for each solvent system) with  $s$  values estimated from bulk copolymerization; as discussed earlier, the  $k_{p, \text{ST}}$  and  $k_{p, \text{HEMA}}$  values in DMF are decreased by 20% and 40% compared to bulk, respectively. The resulting curves are shown as Figure 8a. The change in  $r$  values has a quite significant effect in the  $k_{p, \text{cop}}$  curves calculated for ST/HEMA copolymerization in all the solvents, moving the IPUE predictions for  $k_{p, \text{cop}}$  in toluene above the experimental values, the predictions in DMF below the data, and the predictions in BuOH well below the experimental results. The IPUE can be forced to match the experimental  $k_{p, \text{cop}}$  data by adjusting the  $s$  values for each solvent system, as shown in Figure 8b with the best-fit values summarized in Table 4. While providing a good fit to the data, the need to have solvent-specific

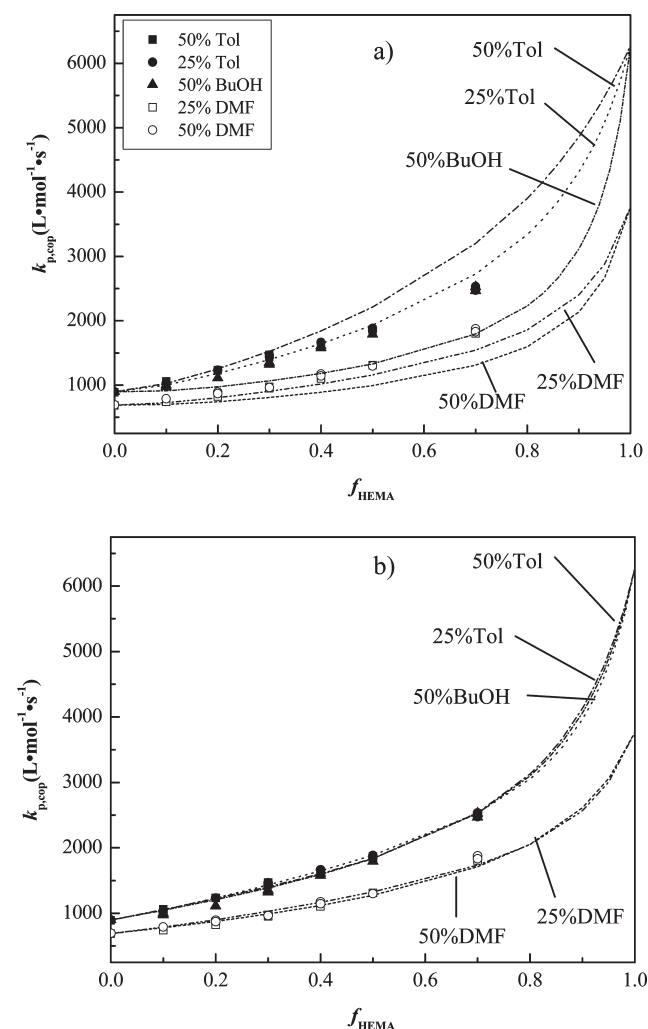


**Figure 8.** IPUE model representation of ST/HEMA solution  $k_{p, \text{cop}}$  data (symbols as in Figure 6a) obtained by PLP/SEC at 90 °C: (a) curves calculated using  $r$  values fit to composition data (Table 3) and estimates for  $s$  from bulk copolymerization ( $s_{\text{ST}} = 0.38$  and  $s_{\text{HEMA}} = 1.34$ ); (b) curves calculated using  $r$  values fit to composition data (Table 3) and  $s$  values fit to each individual data set (Table 4).

**Table 4.** Values of IPUE Reactivity Ratios and Homopropagation Rate Coefficients ( $k_p$ , in  $\text{L} \cdot \text{mol}^{-1} \cdot \text{s}^{-1}$ ) at 90 °C for Copolymerization of Styrene (ST) with 2-Hydroxyethyl Methacrylate (HEMA) in Solution and in Bulk<sup>a</sup>

	bulk <sup>13</sup>	toluene		DMF		butanol
		25 vol %	50 vol %	25 vol %	50 vol %	50 vol %
$r_{\text{ST}}$	$0.27 \pm 0.01$	$0.26 \pm 0.02$	$0.23 \pm 0.02$	$0.35 \pm 0.01$	$0.45 \pm 0.03$	$0.44 \pm 0.03$
$r_{\text{HEMA}}$	$0.49 \pm 0.03$	$0.66 \pm 0.08$	$1.09 \pm 0.18$	$0.49 \pm 0.04$	$0.53 \pm 0.10$	$0.54 \pm 0.10$
$s_{\text{ST}}$	$0.38 \pm 0.01$	$0.47 \pm 0.02$	$0.64 \pm 0.08$	$0.45 \pm 0.02$	$0.47 \pm 0.02$	$0.47 \pm 0.13$
$s_{\text{HEMA}}$	$1.34 \pm 0.71$	$0.35 \pm 0.05$	$0.19 \pm 0.02$	$0.65 \pm 0.22$	<i>n.d.</i>	<i>n.d.</i>
$k_{p, \text{ST}}$	895	895	895	691	691	895
$k_{p, \text{HEMA}}$	6272	6272	6272	3763	3763	6272

<sup>a</sup>*n.d.*: not determined; cannot be estimated.

radical and monomer reactivity ratios to simultaneously describe ST/HEMA copolymer composition and  $k_{p, \text{cop}}$  data is disappointing.

It is interesting to note that the parameter that controls the shape of the ST/HEMA  $k_{p, \text{cop}}$  curve is different for toluene than the polar solvents. It is possible to achieve a reasonable representation of the 50 vol % toluene data with  $s_{\text{ST}}$  fixed at the bulk value of 0.38 and  $s_{\text{HEMA}}$  decreased to 0.35, similar to the curve shown in Figure 8b calculated with the best-fit  $s$  values in Table 4; however, the data cannot be well-represented keeping  $s_{\text{HEMA}}$  fixed and varying  $s_{\text{ST}}$ . The corresponding copolymer composition data measured in toluene were also fit by keeping  $r_{\text{ST}}$  fixed and changing  $r_{\text{HEMA}}$ . The opposite is true for the ST/HEMA  $k_{p, \text{cop}}$  data in DMF and BuOH, which are fit by increasing  $s_{\text{ST}}$  values compared to bulk; similarly, the  $r_{\text{ST}}$  values were varied to fit the ST/HEMA copolymer composition data in DMF and BuOH. For these latter fits, the  $s_{\text{HEMA}}$  values are indeterminate, and thus could be kept at the bulk value of 1.34 without significantly affecting the shape of the curve. Perhaps these systematic variations will provide a means to modify the IPUE to account for specific H-bonding interactions.

## Conclusions

The PLP technique has been employed to systematically investigate free radical solution copolymerization of ST with BMA, GMA, and HEMA at 90 °C. Copolymer composition data, determined via proton NMR, illustrate the solvent effects on monomer reactivity ratios. DMF and *n*-butanol both decrease the reactivity of ST radicals with HEMA, most likely due to the disruption of monomer–monomer hydrogen bonding, while nonpolar toluene increases the reactivity of HEMA radicals toward HEMA compared to ST. Addition of *n*-butanol to the ST/BMA system also significantly affects copolymer composition, increasing the relative addition rate of BMA to a ST radical. However, addition of toluene or DMF to ST/BMA has little or no effect on copolymer composition, a result also seen for ST/GMA copolymerization in all three solvents. From this study it is clear that H-bonding solvents or monomers cause copolymer composition to vary greatly compared to bulk. The terminal model can still be used to represent these composition data, with a systematic variation in monomer reactivity ratios with solvent choice and concentration.

Despite the variation in copolymer composition with solvent choice, the variation of the composition-averaged copolymer propagation rate coefficients,  $k_{p, \text{cop}}$ , with monomer composition is well-described by the implicit penultimate unit effect (IPUE) model using reactivity ratios estimated in bulk, provided that homopropagation end point values are adjusted for solvent effects. (DMF decreases the value of  $k_{p, \text{ST}}$  and  $k_{p, \text{HEMA}}$ ; *n*-butanol increases the value of  $k_{p, \text{BMA}}$ .) The fact that  $s$  and  $r$  values determined in bulk provide a good representation of  $k_{p, \text{cop}}$  curves for H-bonding systems but not copolymer composition is surprising, and will be further explored with a study of copolymerization propagation kinetics and solvent effects of hydroxy-functional monomers in mixed acrylate/methacrylate systems.

**Acknowledgment.** We thank E. I. du Pont de Nemours and Co. and Queen's University for financial support of this work, and Prof. Dr. Sabine Beuermann of Potsdam University for helpful discussions.

**Supporting Information Available:** Table S1–S3 summarizing detailed PLP/SEC and NMR results for ST/GMA,

ST/BMA and ST/HEMA copolymerizations at 90 °C in *n*-butanol, toluene, and DMF solvents. This material is available free of charge via the Internet at <http://pubs.acs.org>.

## References and Notes

- Barb, W. G. *J. Polym. Sci.* **1953**, *10*, 49–62.
- Barb, W. G. *J. Polym. Sci.* **1953**, *11*, 117–126.
- Klumperman, B.; O'Driscoll, K. F. *Polymer* **1993**, *34*, 1032–1037.
- Klumperman, B.; Kraeger, I. R. *Macromolecules* **1994**, *27*, 1529–1534.
- Coote, M. L.; Davis, T. P.; Klumperman, B.; Monteiro, M. J. *Rev. Macromol. Chem. Phys.* **1998**, *38*, 567–593.
- Mayo, F. R.; Lewis, F. M. *J. Am. Chem. Soc.* **1944**, *66*, 1594–1601.
- Harwood, H. J. *Makromol. Chem., Makromol. Symp.* **1987**, *10/11*, 331–354.
- Ito, T.; Otsu, T. *J. Macromol. Sci., Part A: Chem.* **1969**, *3*, 197–203.
- Fujihara, H.; Yamazaki, K.; Matsubara, Y.; Yoshihara, M.; Maeshima, T. *J. Macromol. Sci., Part A: Chem.* **1979**, *13*, 1081–1088.
- Bontà, G.; Gallo, B. M.; Russo, S. *Polymer* **1975**, *16*, 429–432.
- O'Driscoll, K. F.; Monteiro, M. J.; Klumperman, B. *J. Polym. Sci., Part A* **1997**, *35*, 515–520.
- Otsu, T.; Ito, T.; Imoto, M. *J. Polym. Sci., Part A* **1966**, *4*, 733–736.
- Liang, K.; Dossi, M.; Moscatelli, D.; Hutchinson, R. A. *Macromolecules* **2009**, *42*, 7736–7744.
- Wang, W.; Hutchinson, R. A. *Macromolecules* **2008**, *41*, 9011–9018.
- Li, D.; Li, N.; Hutchinson, R. A. *Macromolecules* **2006**, *39*, 4366–4373.
- Lebduška, J.; Šnupárek, J.; Kašpar, K.; Čermák, V. *J. Polym. Sci., Part A: Polym. Chem.* **1986**, *24*, 777–791.
- Schoonbrood, H. A. S.; Aerdt, A. M.; German, A. L.; van der Velden, G. P. M. *Macromolecules* **1995**, *28*, 5518–5525.
- Sánchez-Chaves, M.; Martinez, G.; Madruga, E. J. *J. Polym. Sci., Part A: Polym. Chem.* **1999**, *37*, 2941–2948.
- Merz, E.; Alfrey, T.; Goldfinger, G. *J. Polym. Sci.* **1946**, *1*, 75–82.
- Fukuda, T.; Ma, Y.; Inagaki, H. *Macromolecules* **1985**, *18*, 26–31.
- Buback, M.; Kurz, C. *Macromol. Chem. Phys.* **1998**, *199*, 2301–2310.
- Beuermann, S. *Macromol. Rapid Commun.* **2009**, *30*, 1066–1088.
- Hutchinson, R. A.; Paquet, D. A., Jr.; Beuermann, S.; McMinn, J. H. *Ind. Eng. Chem. Res.* **1998**, *37*, 3567–3574.
- Coote, M. L.; Davis, T. P. *Eur. Polym. J.* **2000**, *36*, 2423–2427.
- Zammit, M. D.; Davis, T. P.; Willett, G. D.; O'Driscoll, K. F. *J. Polym. Sci., Part A: Polym. Chem.* **1997**, *35*, 2311–2321.
- Morrison, B. R.; Piton, M. C.; Winnik, M. A.; Gilbert, R. G.; Napper, D. H. *Macromolecules* **1993**, *26*, 4368–4372.
- Beuermann, S. *Macromolecules* **2004**, *37*, 1037–1041.
- Beuermann, S.; Nelke, D. *Macromol. Chem. Phys.* **2003**, *204*, 460–470.
- Fukuda, T.; Kubo, K.; Ma, Y.-D.; Inagaki, H. *Polym. J. (Tokyo)* **1987**, *19*, 523–530.
- Olaj, O. F.; Schnöll-Bitai, I. *Monatsh. Chem.* **1999**, *130*, 731–740.
- Wang, W.; Hutchinson, R. A. *Macromol. React. Eng.* **2008**, *2*, 199–214.
- Wang, W.; Hutchinson, R. A. *AIChE J.* **2010**, in press.
- Zhang, M.; Ray, W. H. *J. Appl. Polym. Sci.* **2002**, *86*, 1630–1662.
- Hutchinson, R. A.; Beuermann, S.; Paquet, D. A., Jr.; McMinn, J. H.; Jackson, C. *Macromolecules* **1998**, *31*, 1542–1547.
- Hutchinson, R. A.; Beuermann, S.; Paquet, D. A., Jr.; McMinn, J. H.; Jackson, C. *Macromolecules* **1997**, *30*, 3490–3493.
- Polymer Handbook*, 4th ed.; Brandrup, J., Immergut, E. H., Grulke, E. A., Eds.; Wiley-Interscience: New York, 1999.
- Hutchinson, R. A.; Paquet, Jr. D. A.; McMinn, J. H.; Beuermann, S.; Fuller, R. E.; Jackson, C. *5th International Workshop on Polymer Reaction Engineering*; DECHEMA Monographs 131; VCH Publishers: Weinheim, Germany, 1995; pp 467–492.
- Couvreux, L.; Piteau, G.; Castignolles, P.; Tonge, M.; Coutin, B.; Charleux, B.; Vairon, J.-P. *Macromol. Symp.* **2001**, *174*, 197–207.
- Corradini, F.; Marchetti, A.; Tagliazucchi, M.; Tassi, L.; Tosi, G. *Can. J. Chem. Eng.* **1993**, *71*, 124–129.
- Coote, M. L.; Davis, T. P. *Prog. Polym. Sci.* **1999**, *24*, 1217.
- Kamachi, M.; Liaw, D. J.; Nozakura, S. *Polym. J.* **1979**, *12*, 921–928.